Preparation of humulene epoxides

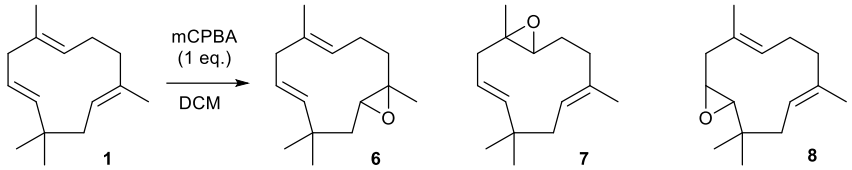

To a solution of humulene **1** (124.0 mg, 0.61 mmol, 1 eq.) in CH_2Cl_2 (6 mL) at –10 °C was added portionwise *m*CPBA (77%, 136.0 mg, 0.61 mmol, 1 eq.). After stirring at –10 °C for 24 h, the reaction mixture was diluted with H_2O (20 mL) and extracted with diethyl ether (3 × 10 mL). The combined organic phases were dried over $MgSO_4$ and then concentrated under reduced pressure. The residue was purified by column chromatography on silica gel (petrol ether / diethyl ether = 6 / 1) to give **8** and a mixture of **6** and **7**. The mixture of **6** and **7** was further purified by preparative HPLC on a chiral stationary phase to give (+)-**6**, (–)-**6**,[1] (+)-**7** and (–)-**7**.[1]

Compound (+)-**6**. TLC (petrol ether / diethyl ether = 5 / 1): R_f = 0.38; yield: 4.0 mg, 0.02 mmol (3%); optical rotation: $[\alpha]_D^{25}$ = +65.5 (*c* 0.41, benzene); GC (HP-5MS): *I* = 1629; ^{1}H-NMR and ^{13}C-NMR see Table S1.

Compound (–)-**6**. TLC (petrol ether / diethyl ether = 5 / 1): R_f = 0.38; yield: 4.0 mg, 0.02 mmol (3%); optical rotation: $[\alpha]_D^{25}$ = –45.9 (*c* 0.47, benzene), lit: $[\alpha]_D$ = –22.8 ($CHCl_3$);[1] GC (HP-5MS): *I* = 1629; ^{1}H-NMR and ^{13}C-NMR see Table S1.

Compound (+)-**7**. TLC (petrol ether / diethyl ether = 5 / 1): R_f = 0.38; yield: 30 mg, 0.14 mmol (22%); optical rotation: $[\alpha]_D^{25}$ = +95.9 (*c* 0.15, benzene); GC (HP-5MS): *I* = 1641; ^{1}H-NMR and ^{13}C-NMR see Table S2.

Compound (–)-**7**. TLC (petrol ether / diethyl ether = 5 / 1): R_f = 0.38; yield: 30 mg, 0.14 mmol (22%); optical rotation: $[\alpha]_D^{25}$ = –106.3 (*c* 0.14, benzene), lit: $[\alpha]_D$ = –31.2 ($CHCl_3$);[1] GC (HP-5MS): *I* = 1641; ^{1}H-NMR and ^{13}C-NMR see Table S2.

Compound **8**. TLC (petrol ether / diethyl ether = 5 / 1): R_f = 0.71; yield: 7.0 mg, 0.03 mmol (5%); GC (HP-5MS): *I* = 1665; ^{1}H-NMR and ^{13}C-NMR see Table S3.

HPLC

Analytical scale HPLC seperation was carried out using an Azura series HPLC system (Knauer, Berlin, Germany), equipped with DAD 6.1L photodiode array detector (190–1020 nm) and a Daicel (Tokyo, Japan) Chiralpak IC-U column (1.6 μm; 3.0 mm × 100 mm) using an isocratic solvent mixture of [*n*-heptane / 2-propanol (98:2)] with 0.85 mL min^{-1} (352 bar). The UV–Vis absorption was monitored at 210 nm.

Preparative scale HPLC purification was performed on an Azura series HPLC system (Knauer, Berlin, Germany) with a multi wavelength detector MWL 2.1L (190–700 nm) using a YMC ChiralART Cellulose-SC column (5 μm, 250 × 20 mm). The solvent mixture [*n*-heptane / 2-propanol (98:2)] was used at 18.0 mL min^{-1} (44 bar) and monitoring was conducted at 210 nm.

NMR spectroscopy

NMR spectra were recorded at 298 K on a Bruker (Billerica, MA, USA) Avance III HD Cryo (700 MHz) NMR spectrometer. Spectra were measured in C_6D_6 and referenced against solvent signals (^{1}H-NMR, residual proton signal: δ = 7.16 ppm; ^{13}C-NMR: δ = 128.06 ppm).[2]

GC/MS analyses

GC/MS analyses were carried out using a 7890B GC equipped with a HP5-MS fused silica capillary column (30 m, 0.25 mm i. d., 0.50 μm film) and connected to a 5977A mass detector

(Agilent). GC parameters: 1) temperature program: 5 min at 50 °C increasing at 5 °C min^{-1} to 320 °C, 2) injection volume: 2 μL, 3) split ratio: 10:1, 60 s valve time, and 4) carrier gas: He at 1 mL min^{-1}. Retention indices (*I*) were determined from a homologous series of *n*-alkanes (C_7-C_{40}). MS parameters: 1) inlet pressure: 77.1 kPa, He at 23.3 mL min^{-1}, 2) transfer line: 250 °C, and 3) electron energy: 70 eV.

Optical rotations

Optical rotations were recorded on a Modular Compact Polarimeter MCP 100 (Anton Paar, Graz, Austria). The temperature setting was 25 °C; the wavelength of the light used was 589 nm (the sodium D line); the path-length was 10 cm, the compound concentrations *c* are given in g 100 mL^{-1}.

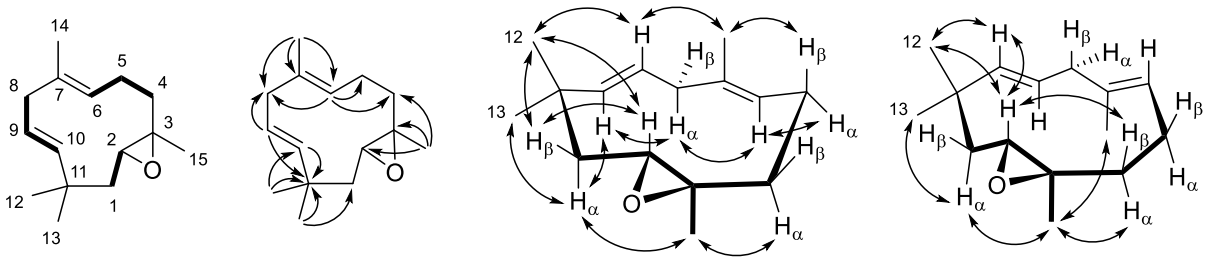

Figure S1. Structure elucidation of **6**. Bold lines: COSY correlations, single headed arrows: key HMBC correlations, double headed arrows: key NOESY correlations. The observed NOESY correlations point to the presence of several conformers.

Table S1. NMR data of humulene epoxide I (**6**) in C_6D_6 recorded at 298 K.

C[a]	type	^{1}H[b]	^{13}C[b]
1	CH_2	1.65 (d, *J* = 14.2, H_β)	41.78
		1.36 (dd, *J* = 14.2, 9.8, H_α)	
2	CH	2.53 (d, *J* = 9.6)	62.87
3	C_q	–	60.62
4	CH_2	2.02 (m, H_α)	39.12
		1.15 (ddd, *J* = 12.4, 12.4, 5.6, H_β)	
5	CH_2	2.01 (m, H_β)	23.75
		1.91 (m, H_α)	
6	CH	5.06 (br dd, *J* = 8.9, 6.5)	126.66
7	C_q	–	139.06
8	CH_2	2.44 (d, *J* = 7.3, 2H)	39.90
9	CH	5.60 (ddd, *J* = 15.8, 7.2, 7.2)	128.25
10	CH	5.24 (d, *J* = 15.8)	141.66
11	C_q	–	35.11
12	CH_3	0.93 (s)	30.79
13	CH_3	1.04 (s)	23.87
14	CH_3	1.50 (br s)	18.10
15	CH_3	1.08 (s)	16.37

[a] Carbon numbering as shown in Figure S1. [b] Chemical shifts δ in ppm, multiplicity: s = singlet, d = doublet, m = multiplet, br = broad, coupling constants *J* are given in Hertz.

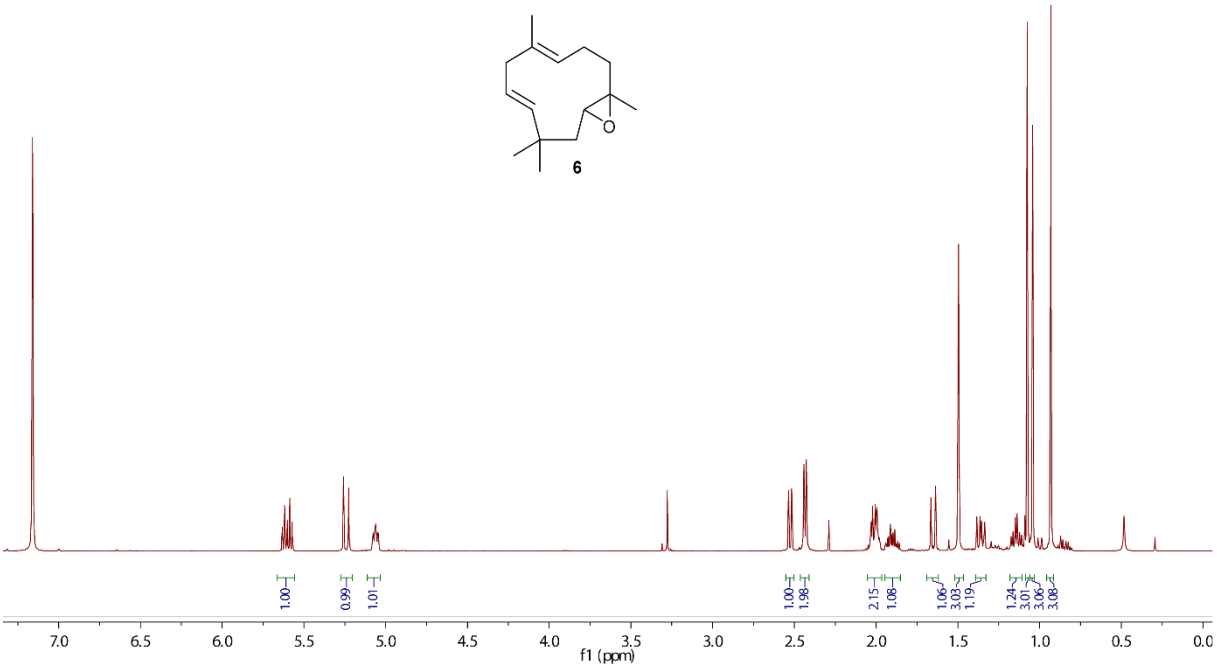

Figure S2. ^{1}H-NMR spectrum of **6** (700 MHz, C_6D_6).

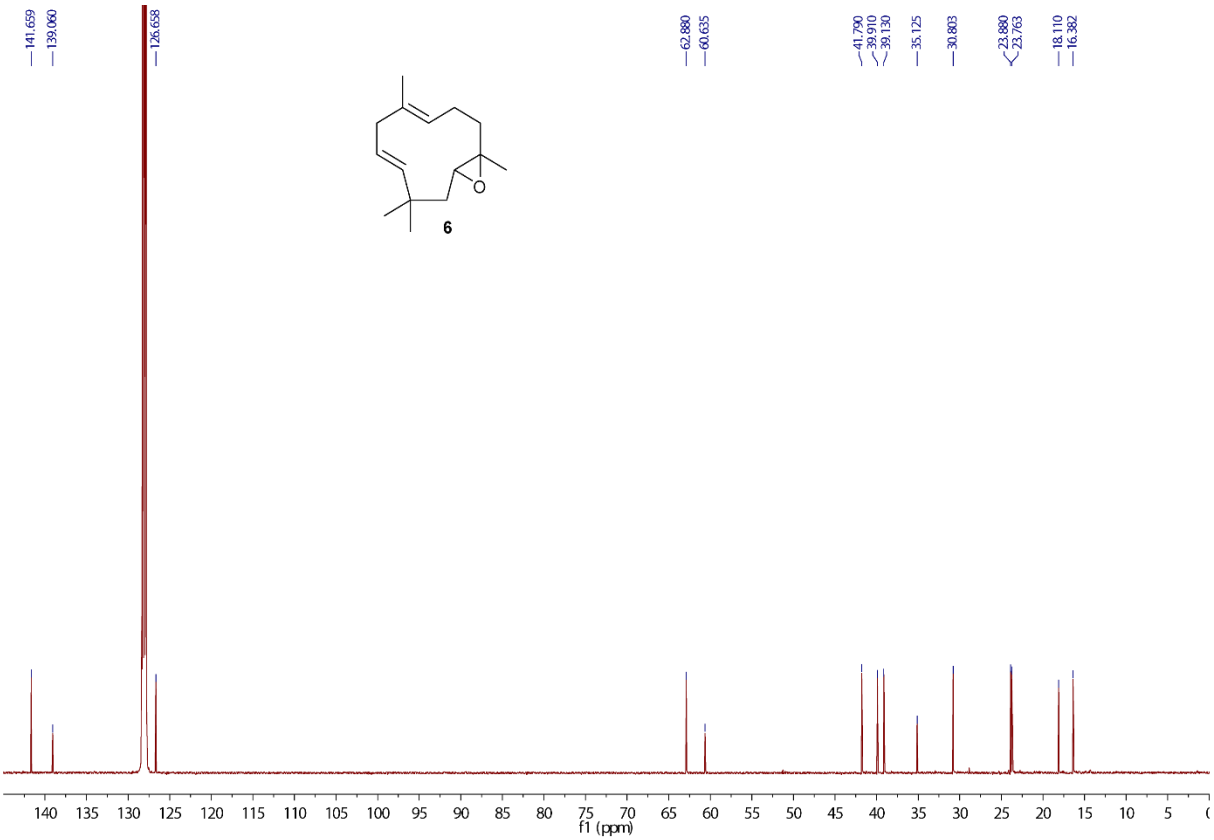

Figure S3. ^{13}C-NMR spectrum of **6** (176 MHz, C_6D_6).

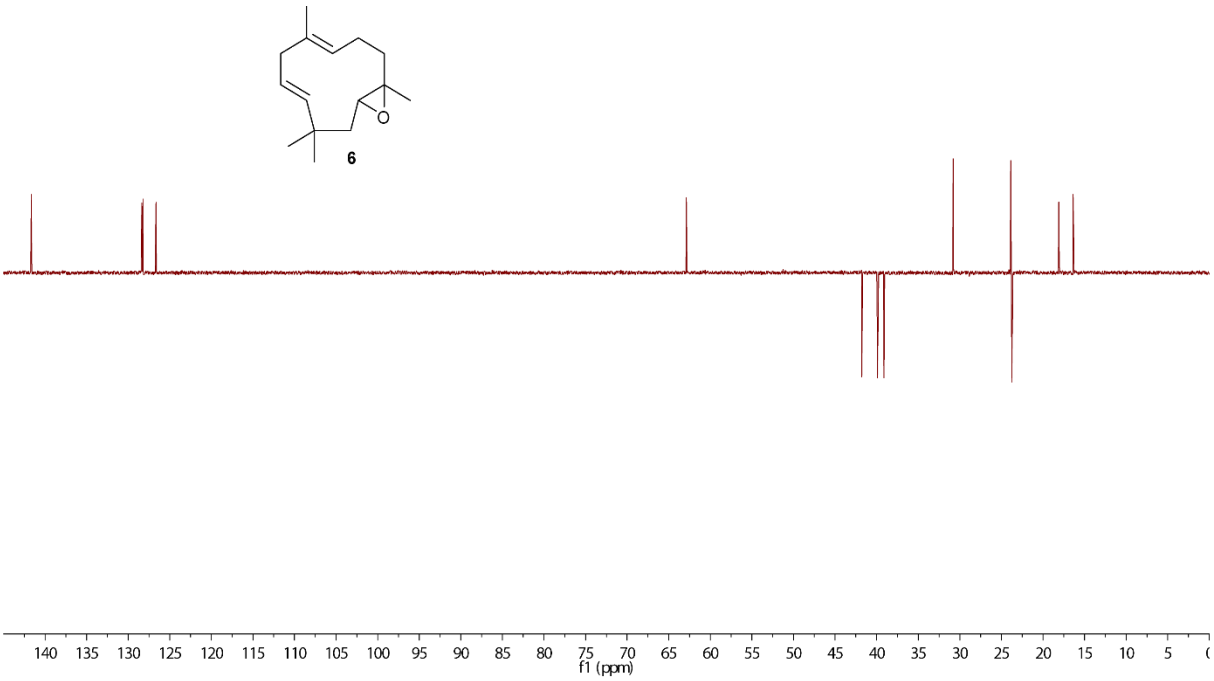

Figure S4. ^{13}C-DEPT spectrum of **6** (176 MHz, C_6D_6).

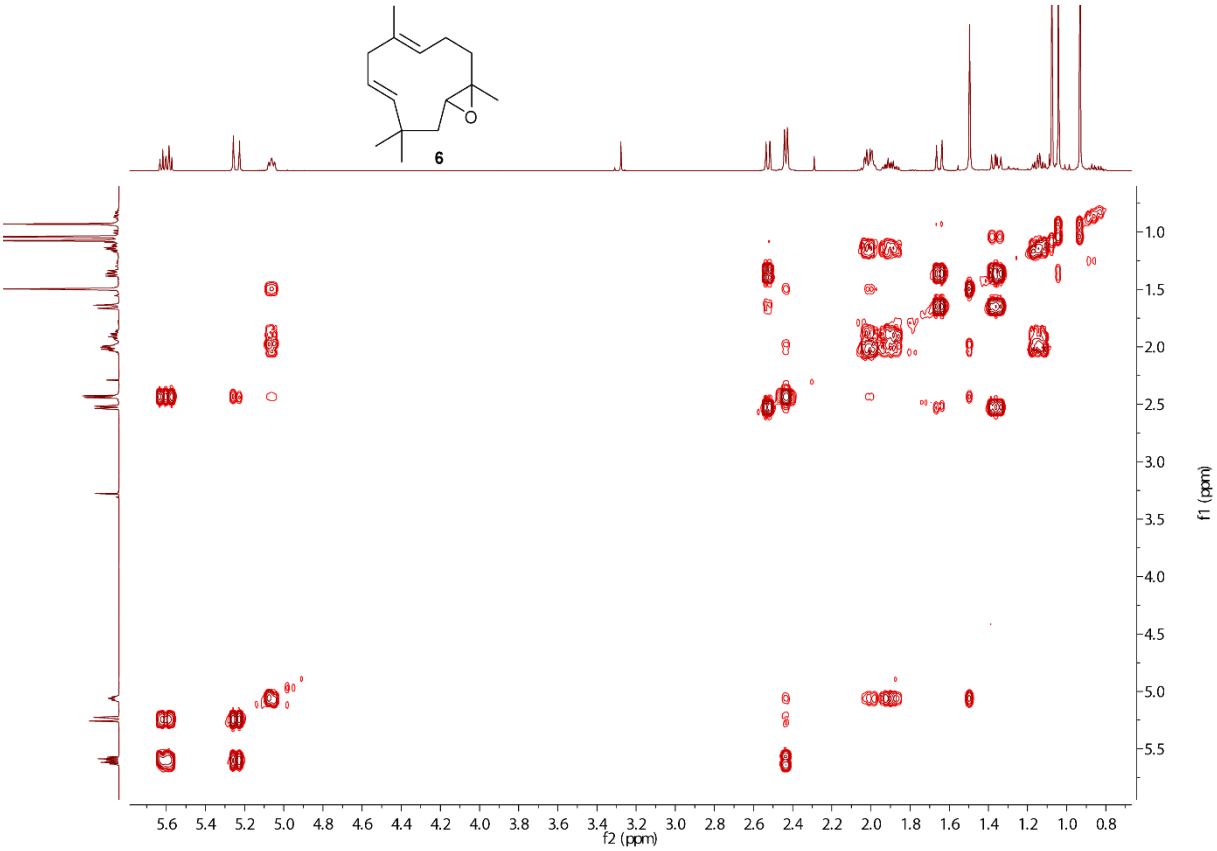

Figure S5. ^{1}H-^{1}H COSY spectrum of **6** (700 MHz, C_6D_6).

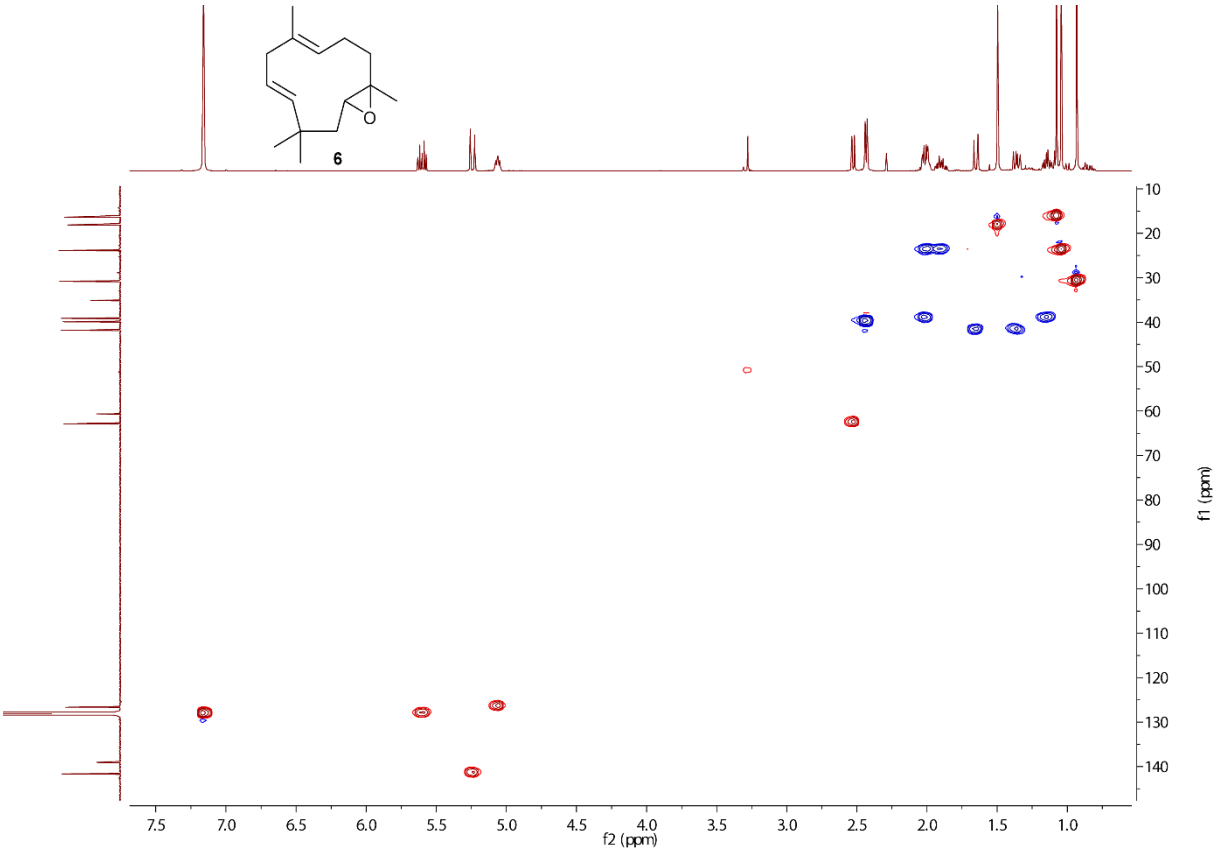

Figure S6. HSQC spectrum of **6** (C_6D_6).

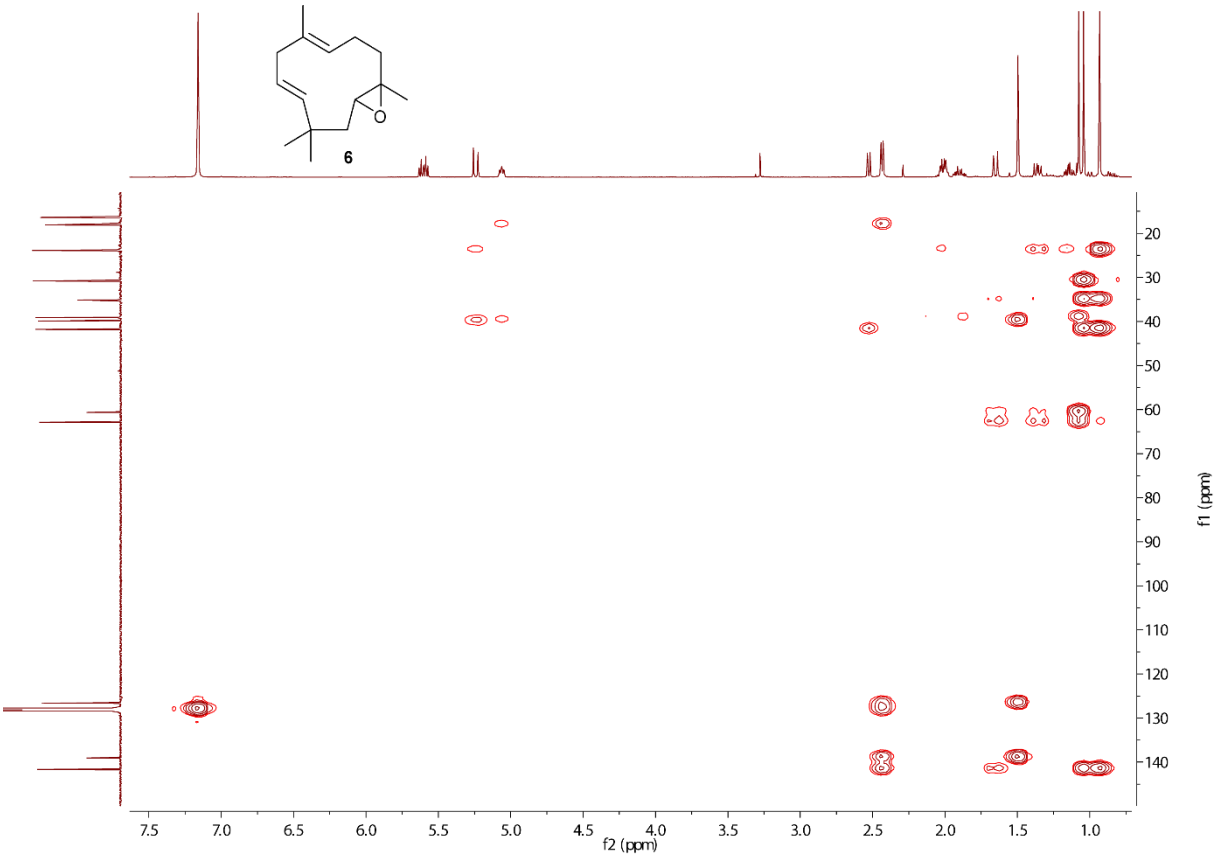

Figure S7. HMBC spectrum of **6** (C_6D_6).

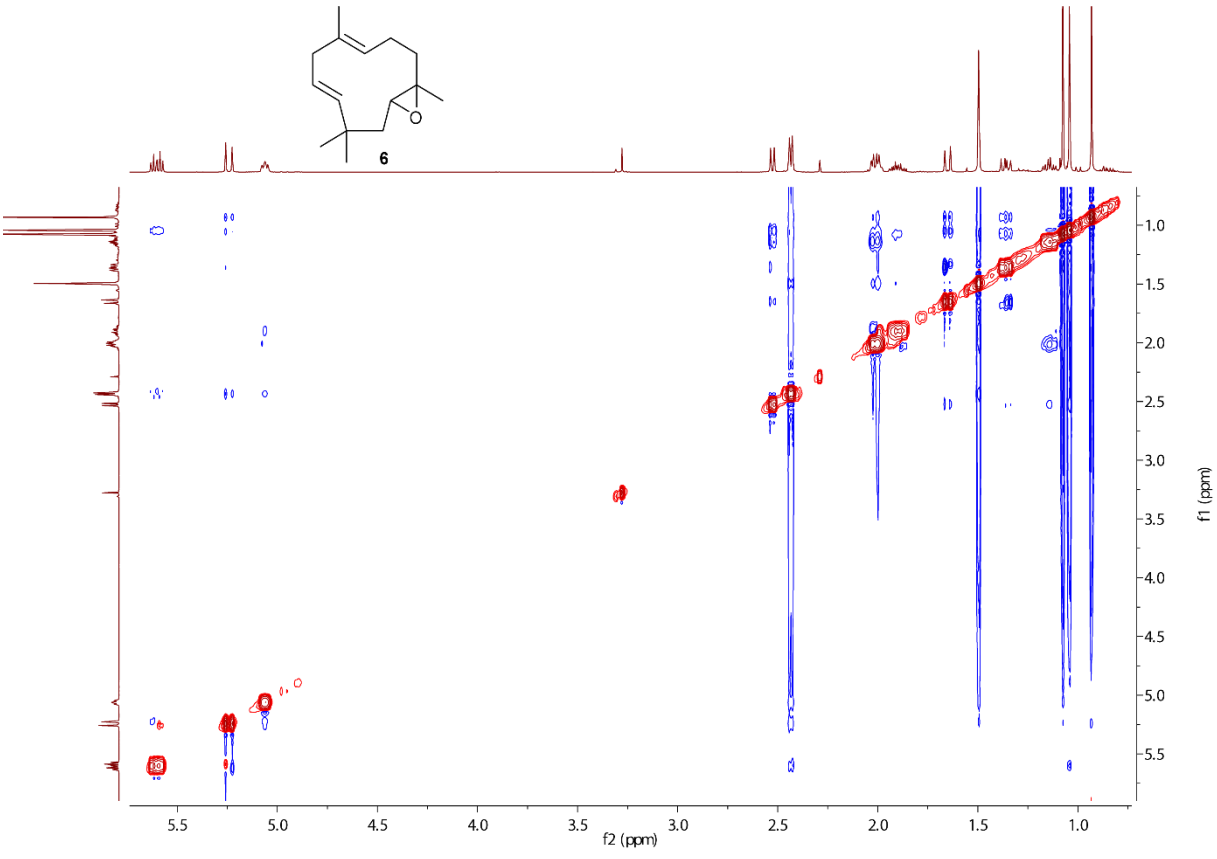

Figure S8. NOESY spectrum of **6** (C_6D_6).

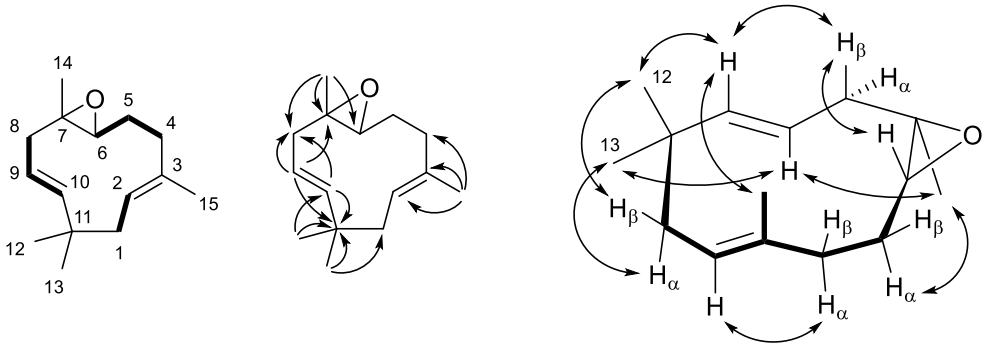

Figure S9. Structure elucidation of **7**. Bold lines: COSY correlations, single headed arrows: key HMBC correlations, double headed arrows: key NOESY correlations.

Table S2. NMR data of humulene epoxide II (**7**) in C_6D_6 recorded at 298 K.

C[a]	type	^{1}H[b]	^{13}C[b]
1	CH_2	1.87 (dd, *J* = 13.6, 9.0, H_β)	40.59
		1.77 (br dd, *J* = 13.7, 5.9, H_α)	
2	CH	4.88 (m)	125.76
3	C_q	–	132.01
4	CH_2	2.00 (m, H_β)	36.99
		1.93 (m, H_α)	
5	CH_2	2.01 (m, H_β)	25.28
		1.26 (m, H_α)	
6	CH	2.39 (dd, *J* = 10.1, 3.6)	61.23
7	C_q	–	62.51
8	CH_2	2.47 (dd, *J* = 12.5, 5.4, H_α)	43.02
		1.69 (dd, *J* = 12.5, 10.5, H_β)	
9	CH	5.12 (ddd, *J* = 15.9, 10.1, 5.3)	122.94
10	CH	4.96 (d, *J* = 16.0)	142.64
11	C_q	–	36.47
12	CH_3	0.98 (s)	29.06
13	CH_3	1.01 (s)	25.83
14	CH_3	1.13 (br s)	17.49
15	CH_3	1.34 (br s)	15.06

[a] Carbon numbering as shown in Figure S9. [b] Chemical shifts δ in ppm, multiplicity: s = singlet, d = doublet, m = multiplet, br = broad, coupling constants *J* are given in Hertz.

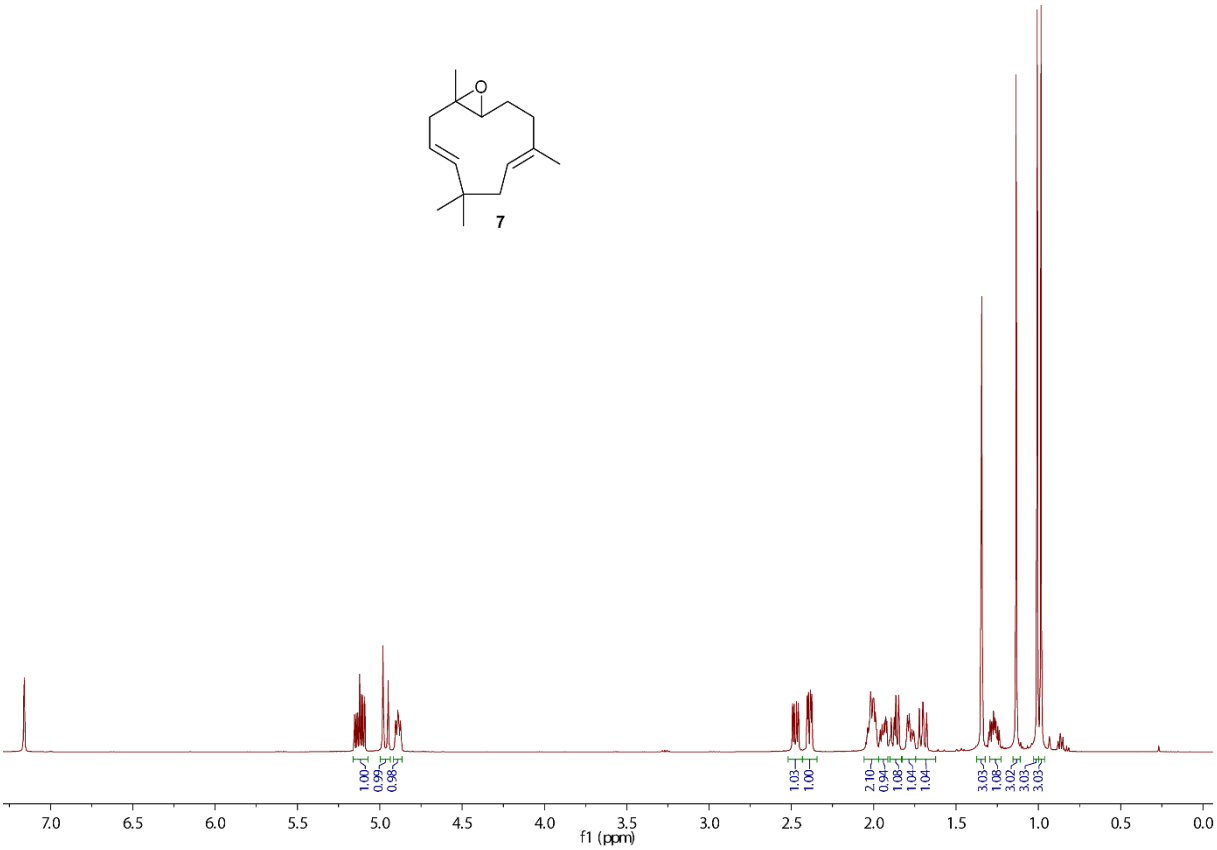

Figure S10. ^{1}H-NMR spectrum of **7** (700 MHz, C_6D_6).

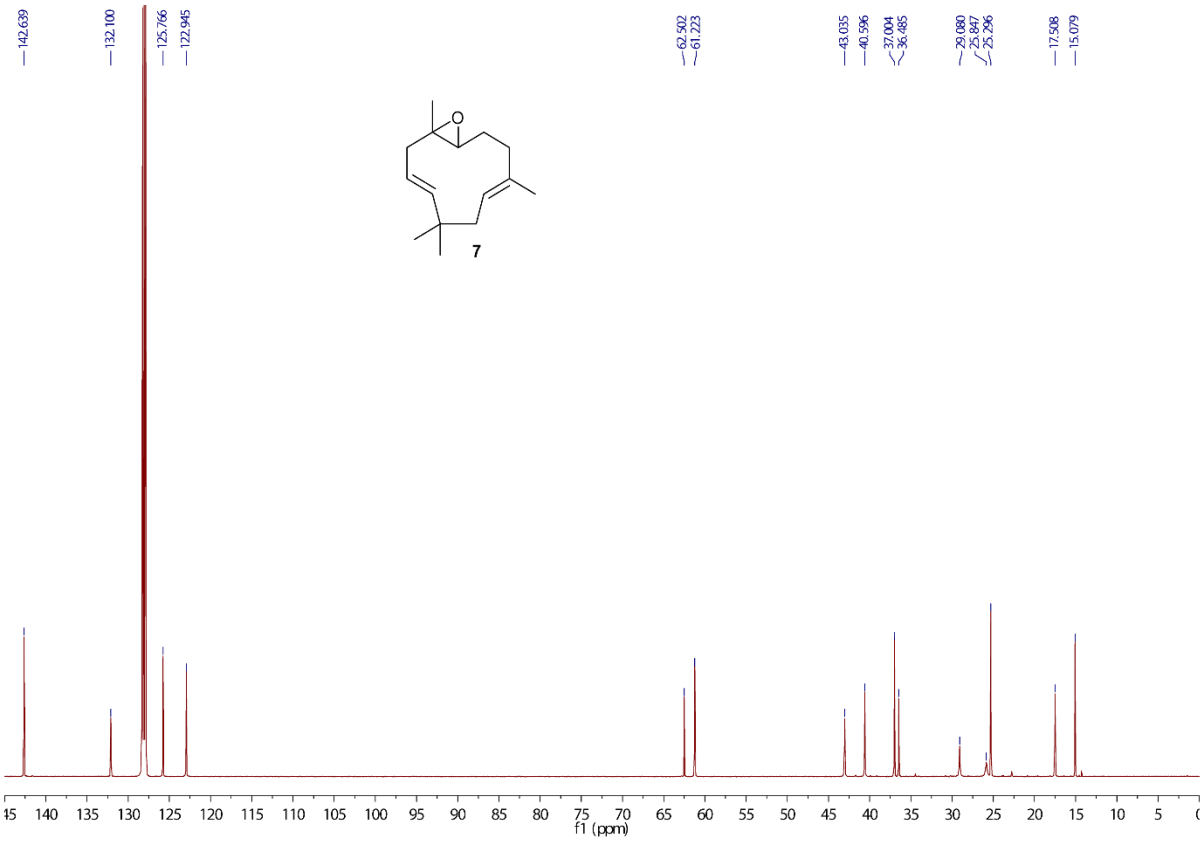

Figure S11. ^{13}C-NMR spectrum of **7** (176 MHz, C_6D_6).

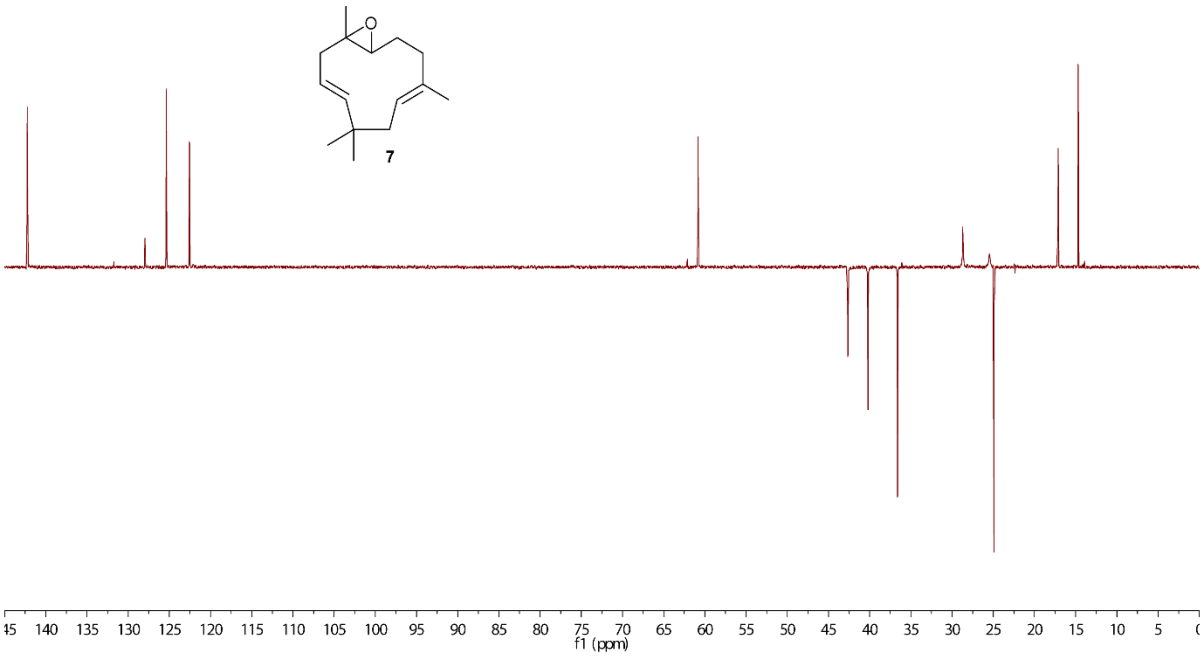

Figure S12. ^{13}C-DEPT spectrum of **7** (176 MHz, C_6D_6).

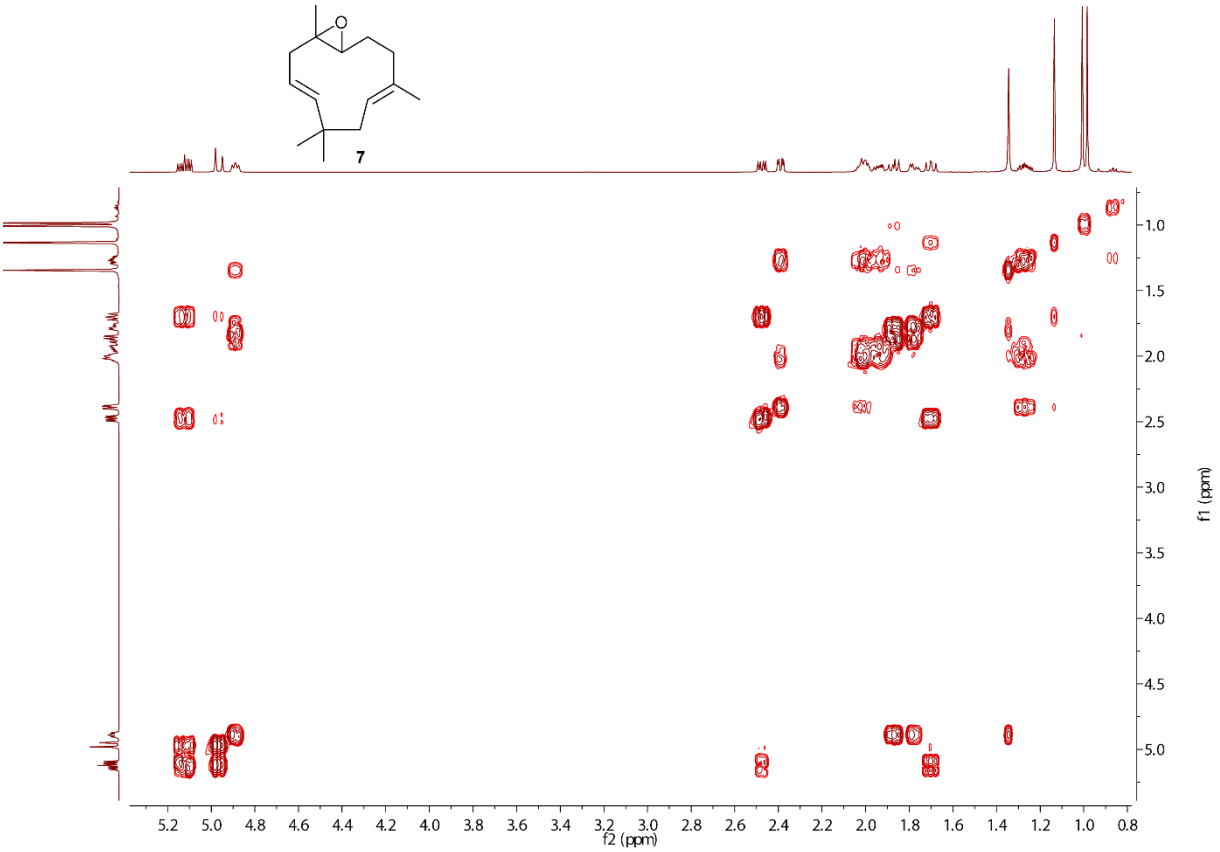

Figure S13. ^{1}H-^{1}H COSY spectrum of **7** (700 MHz, C_6D_6).

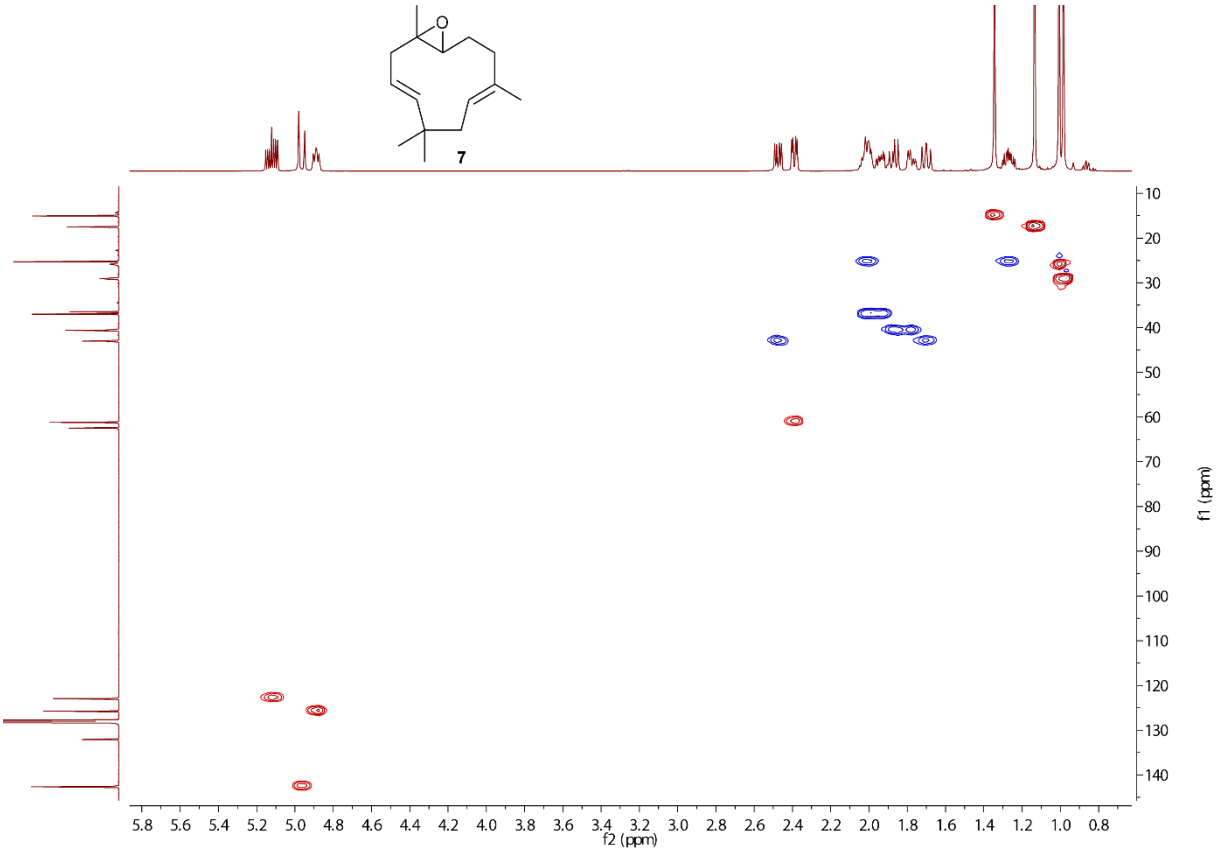

Figure S14. HSQC spectrum of **7** (C_6D_6).

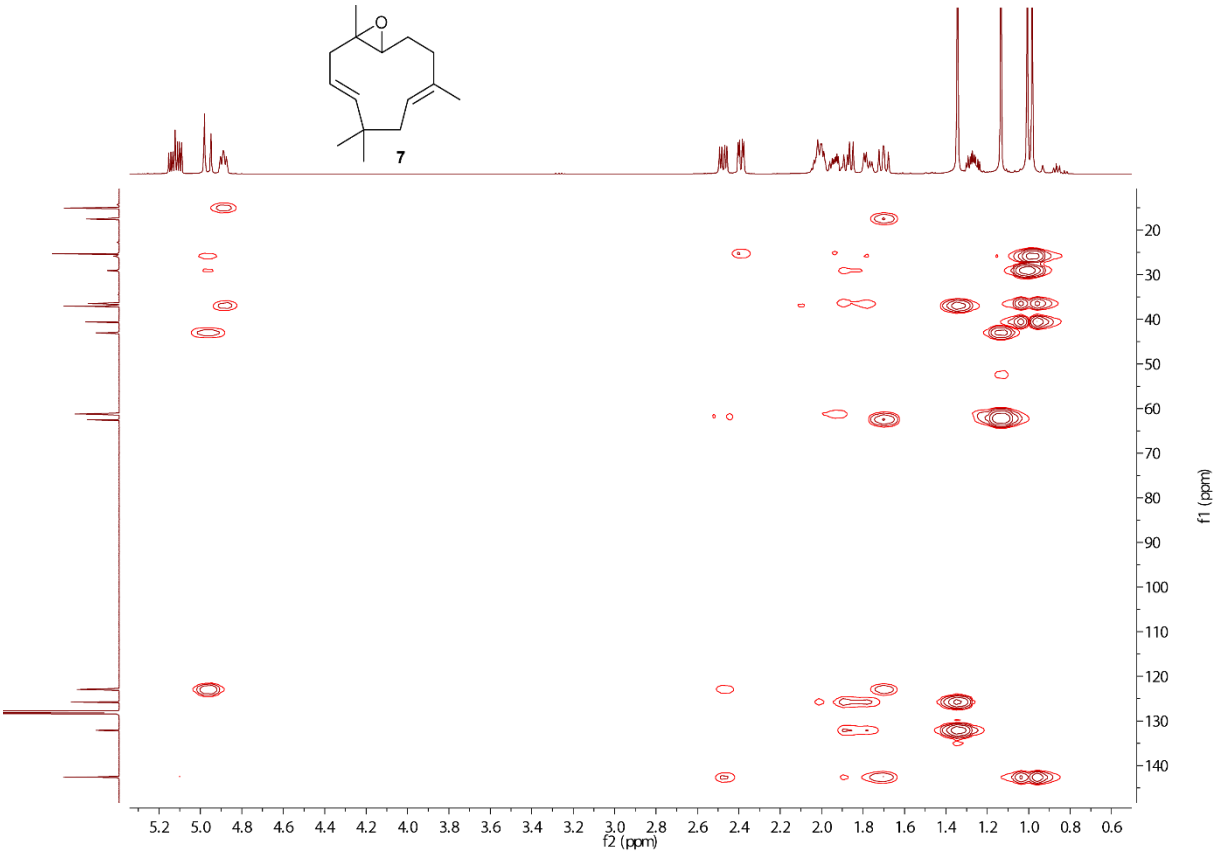

Figure S15. HMBC spectrum of **7** (C_6D_6).

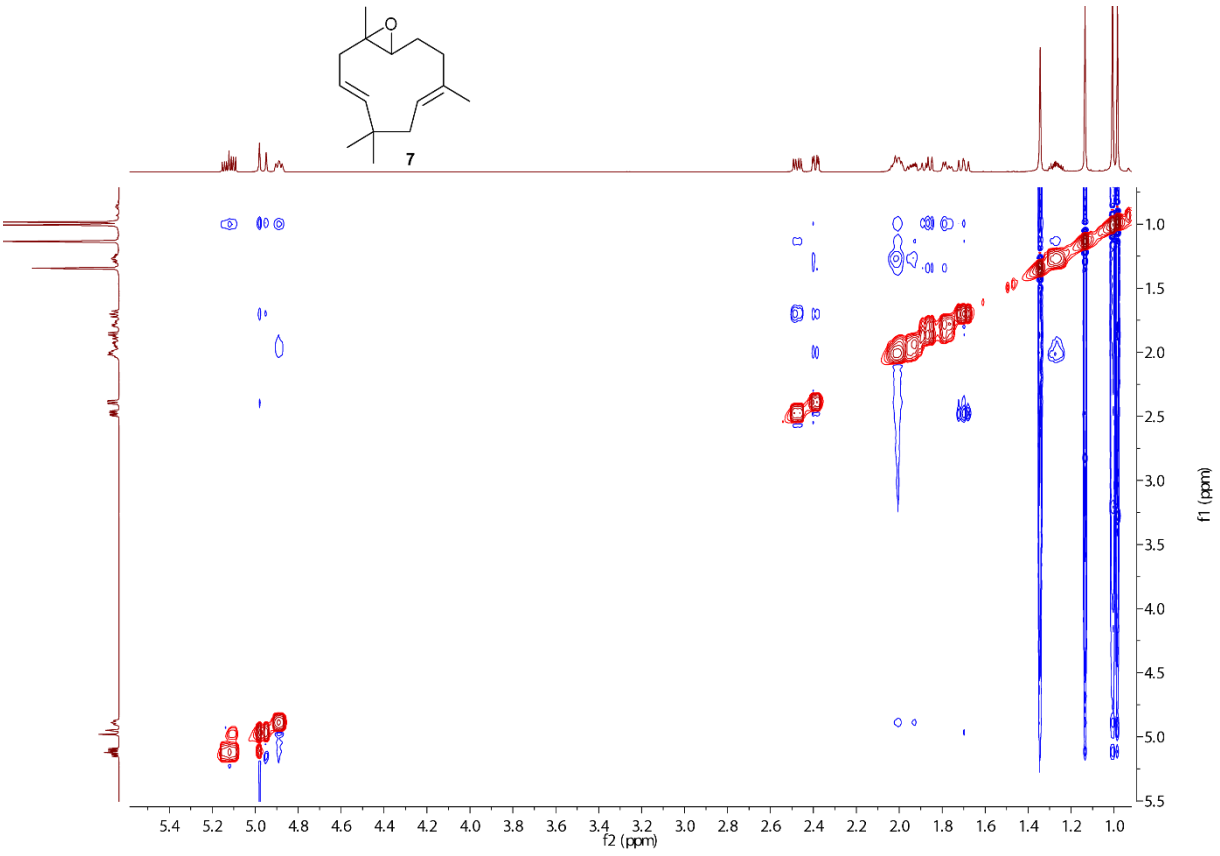

Figure S16. NOESY spectrum of **7** (C_6D_6).

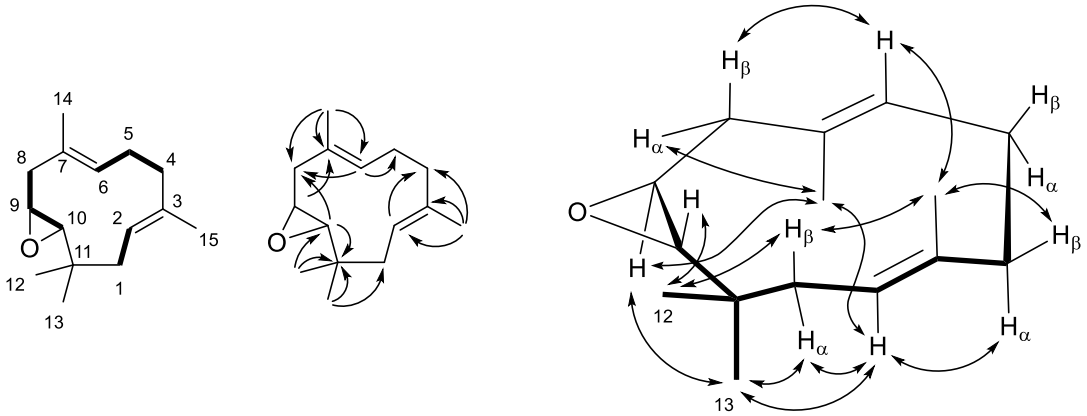

Figure S17. Structure elucidation of **8**. Bold lines: COSY correlations, single headed arrows: key HMBC correlations, double headed arrows: key NOESY correlations.

Table S3. NMR data of humulene epoxide III (**8**) in C_6D_6 recorded at 298 K.

C[a]	type	^{1}H[b]	^{13}C[b]
1	CH_2	2.11 (dd, *J* = 14.6, 10.8, H_β)	39.62
		1.79 (dm, *J* = 14.6, H_α)	
2	CH	4.87 (br dd, *J* = 7.1, 7.1)	123.63
3	C_q	–	133.41
4	CH_2	2.02 (m, H_β)	39.51
		1.91 (m, H_α)	
5	CH_2	1.99 (m, 2H)	23.72
6	CH	4.81 (dm, *J* = 10.4)	126.47
7	C_q	–	132.12
8	CH_2	2.64 (dd, *J* = 12.8, 4.2, H_α)	42.49
		1.54 (dd, *J* = 12.8, 9.4, H_β)	
9	CH	2.80 (ddd, *J* = 9.5, 4.3, 2.3)	56.53
10	CH	2.19 (d, *J* = 2.3)	64.79
11	C_q	–	34.59
12	CH_3	1.10 (s)	29.15
13	CH_3	0.74 (s)	19.28
14	CH_3	1.40 (br s)	17.84
15	CH_3	1.36 (dd, *J* = 1.4, 1.4)	15.36

[a] Carbon numbering as shown in Figure S17. [b] Chemical shifts δ in ppm, multiplicity: s = singlet, d = doublet, m = multiplet, br = broad, coupling constants *J* are given in Hertz.

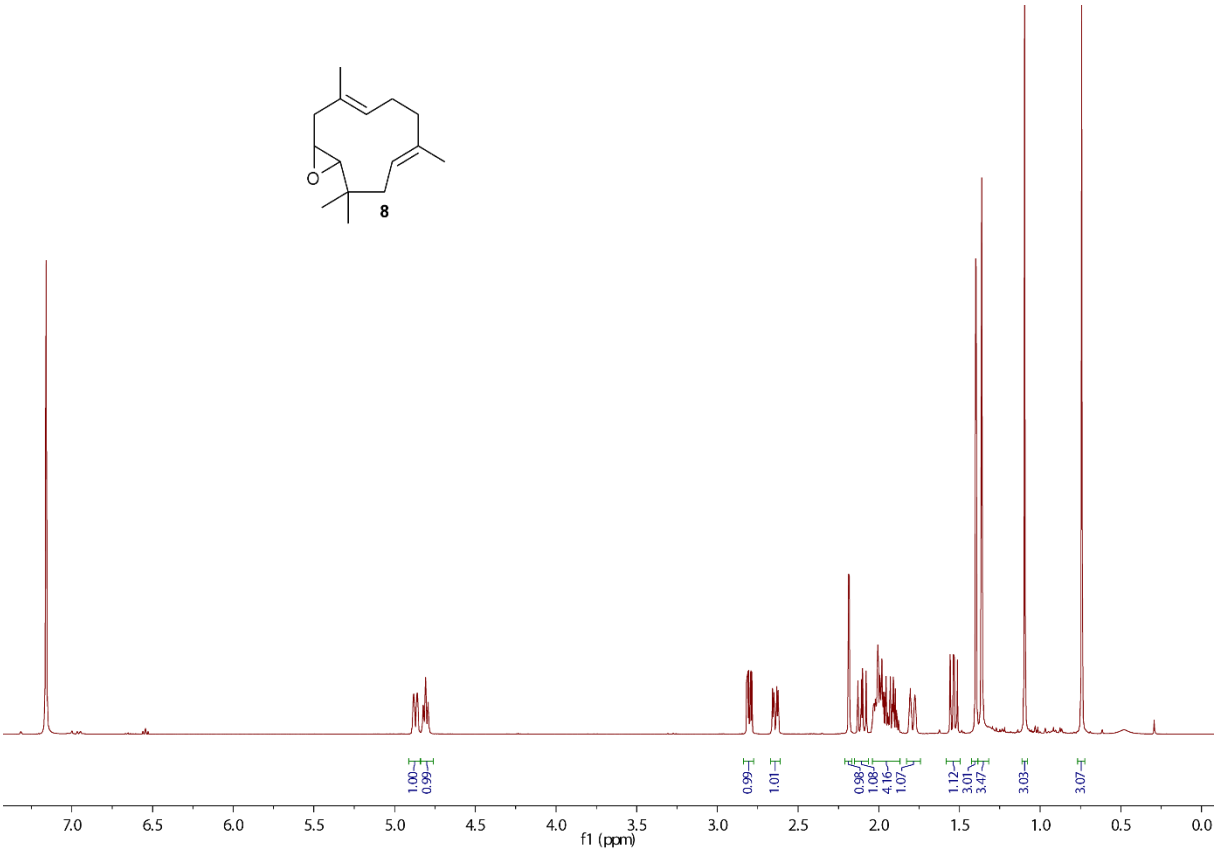

Figure S18. ^{1}H-NMR spectrum of **8** (700 MHz, C_6D_6).

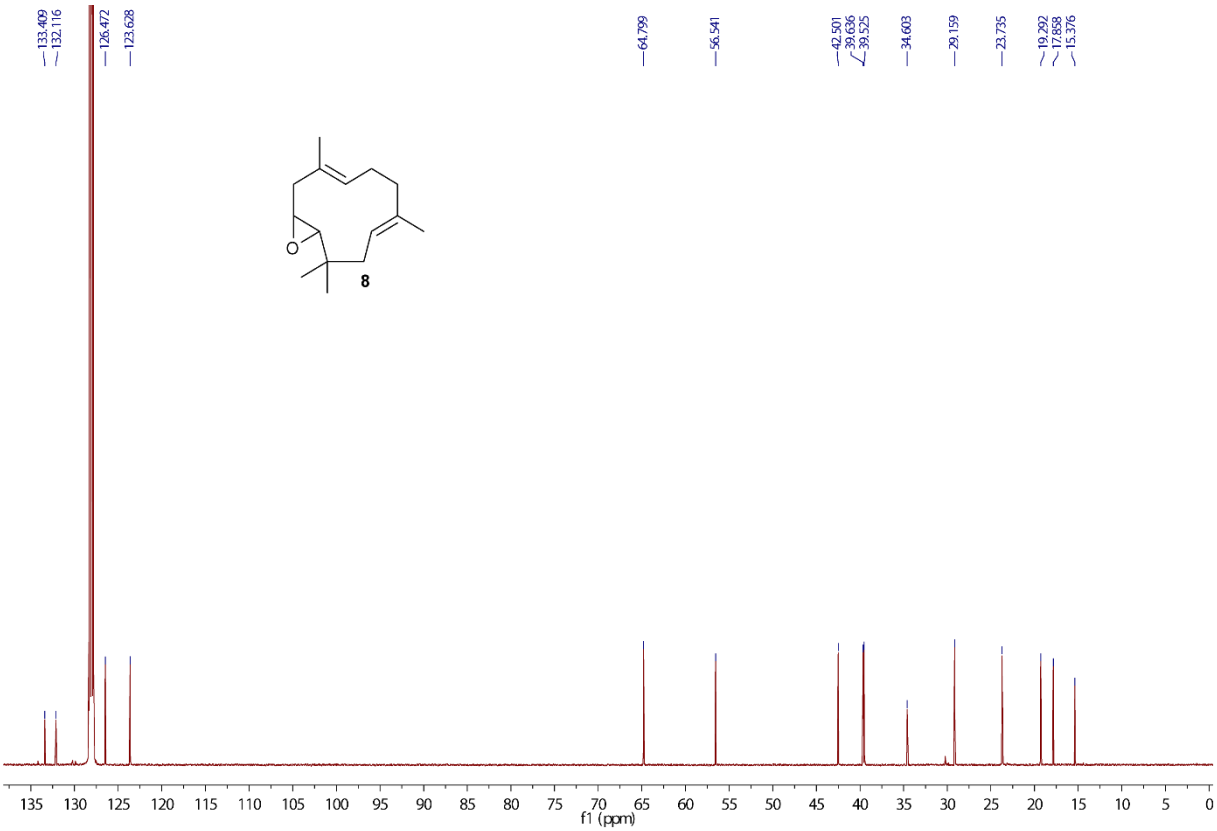

Figure S19. ^{13}C-NMR spectrum of **8** (176 MHz, C_6D_6).

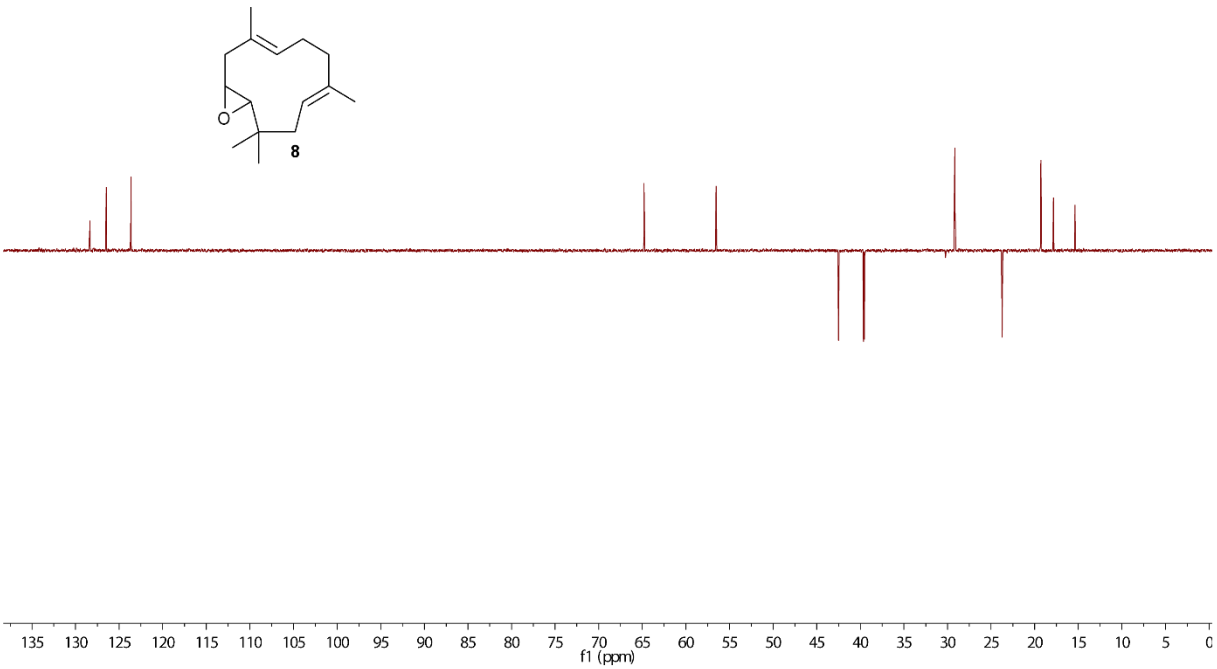

Figure S20. ^{13}C-DEPT spectrum of **8** (176 MHz, C_6D_6).

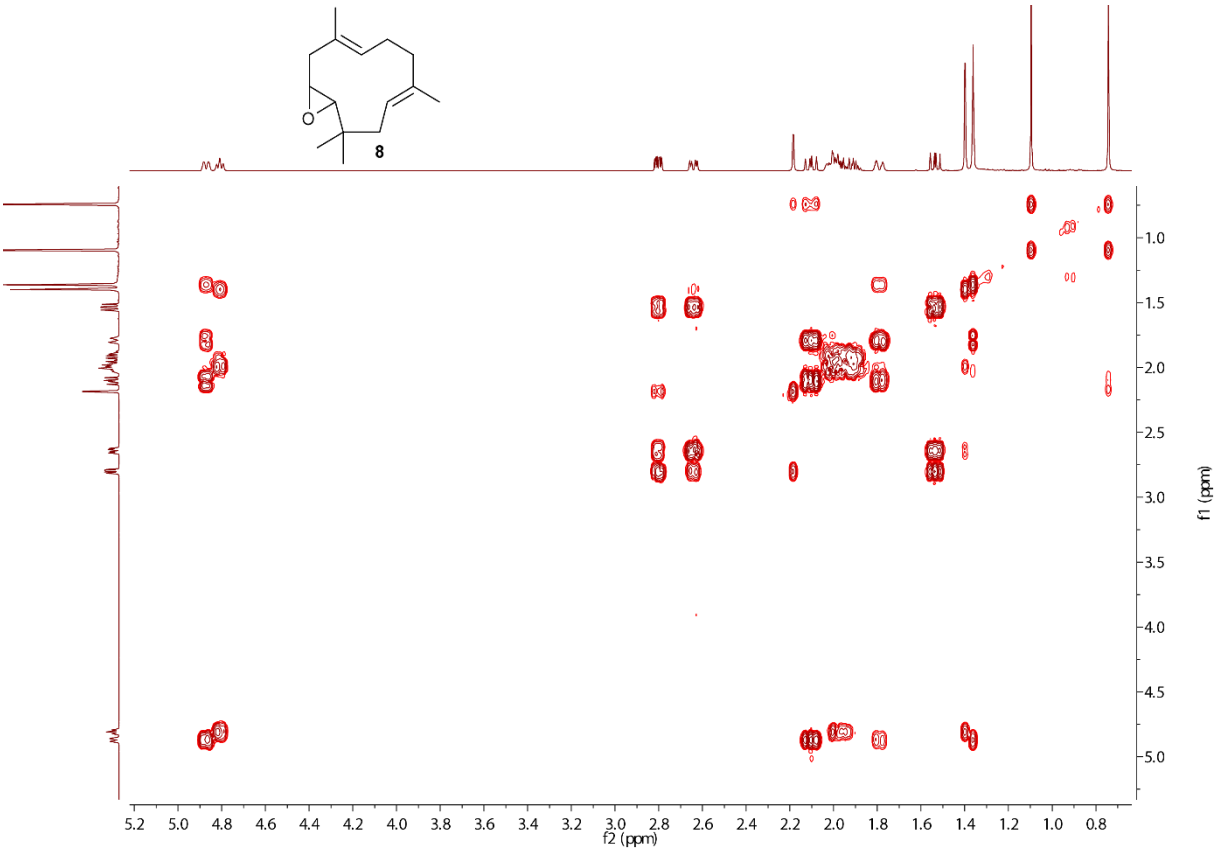

Figure S21. ^{1}H-^{1}H COSY spectrum of **8** (700 MHz, C_6D_6).

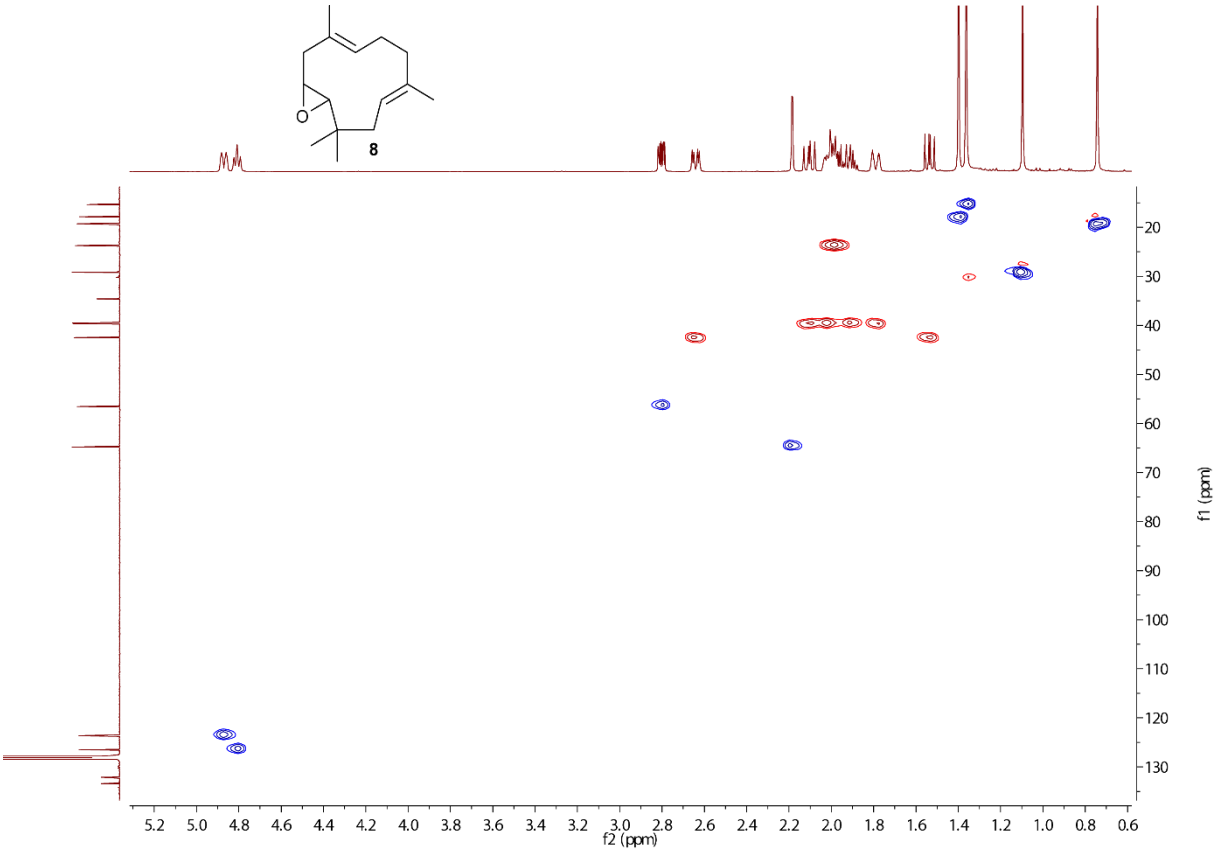

Figure S22. HSQC spectrum of **8** (C_6D_6).

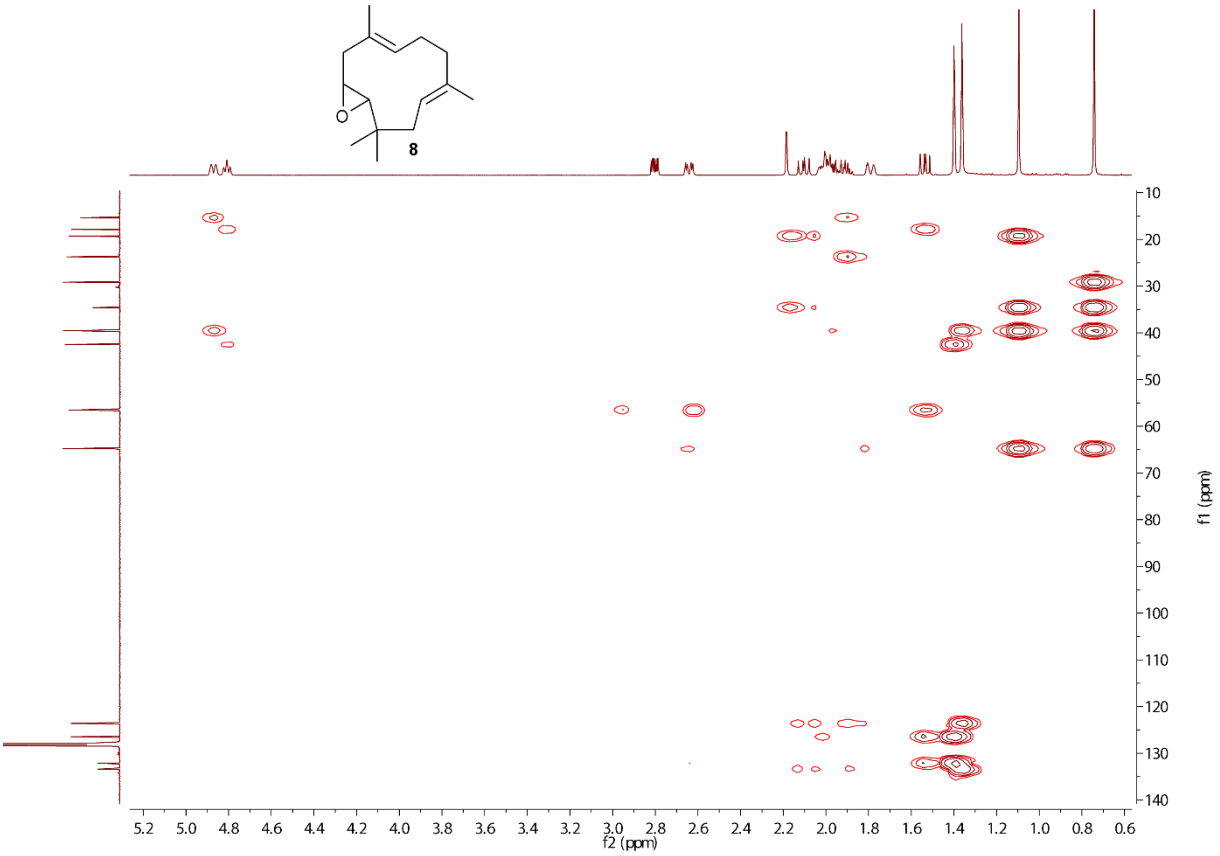

Figure S23. HMBC spectrum of **8** (C_6D_6).

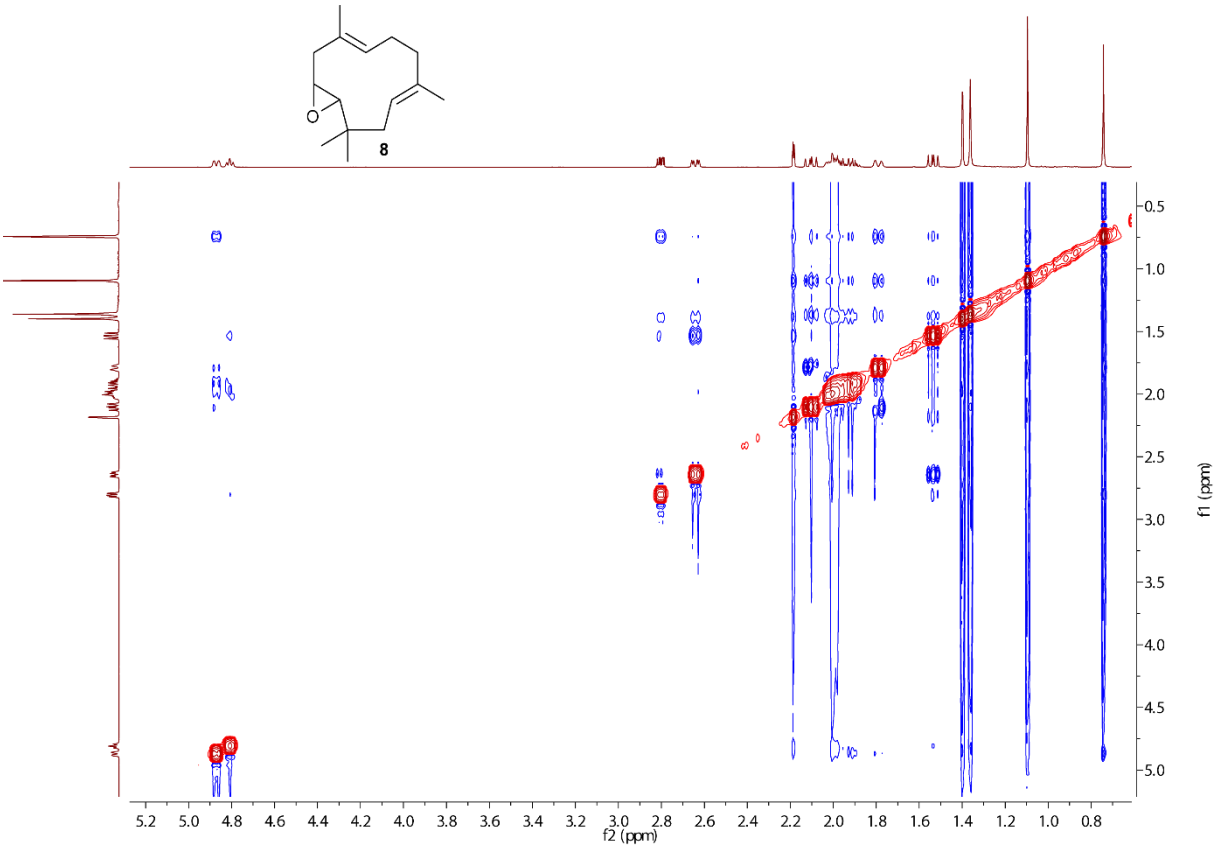

Figure S24. NOESY spectrum of **8** (C_6D_6).

Isotopic labelling experiments

Isotopic labelling experiments were performed with the substrates and enzymes as listed in Table S4.

For the reactions entries 1 – 4, the reaction mixtures contained substrates (5 mg each) in aqueous NH_4HCO_3 solution (2 mL, 25 mM), enzyme elution fractions (5 mL each) purified as reported[3] and incubation buffer (13 mL, 50 mM Tris, 10 mM $MgCl_2$, 20 vol-% glycerol, pH 8.2). After incubation with shaking at 28 °C overnight, the reaction mixtures were extracted with diethyl ether (50 mL). α-Humulene (30 mg) was added and the solvent was evaporated, followed by conversion with mCPBA into epoxides and separation of stereoisomers by HPLC on a chiral stationary phase to obtain (1*S*,6*S*,7*S*)-[1-^{13}C,1-^{2}H]-**7** and (1*S*,6*R*,7*R*)-[1-^{13}C,1-^{2}H]-**7** from experiment 1, (1*R*,6*S*,7*S*)-[1-^{13}C,1-^{2}H]-**7** and (1*R*,6*R*,7*R*)-[1-^{13}C,1-^{2}H]-**7** from experiment 2, (6*S*,7*S*,11*R*)-[12-^{13}C]-**7** and (6*R*,7*R*,11*R*)-[12-^{13}C]-**7** from experiment 3, and (6*S*,7*S*,11*S*)-[12-^{13}C]-**7** and (6*R*,7*R*,11*S*)-[12-^{13}C]-**7** from experiment 4. All products were analysed by NMR spectroscopy.

For the reactions entries 5 and 6, the reaction mixtures contained substrates (0.5 mg each) in aqueous NH_4HCO_3 solution (0.1 mL, 25 mM), enzyme elution fractions (0.2 mL each) and incubation buffer (0.5 mL). After incubation with shaking at 28 °C for 5 h, the reaction mixtures were extracted with *n*-hexane (0.15 mL). The extracts were dried over $MgSO_4$ and analysed by GC-MS.

Table S4. Labelling experiments with AsR6.

entry	substrate	enzymes	results shown in
1	(*R*)-(1-^{13}C,1-^{2}H)FPP[4]	AsR6[5]	Figure S25
2	(*S*)-(1-^{13}C,1-^{2}H)FPP[4]	AsR6	Figure S25
3	(12-^{13}C)FPP[6]	AsR6	Figure S26
4	(13-^{13}C)FPP[6]	AsR6	Figure S26
5	(*R*)-(1-^{2}H)IPP[6]	IDI,[8] FPPS,[9] AsR6	Figure S27
6	(*S*)-(1-^{2}H)IPP[7]	IDI, FPPS, AsR6	Figure S27

A) unlabelled

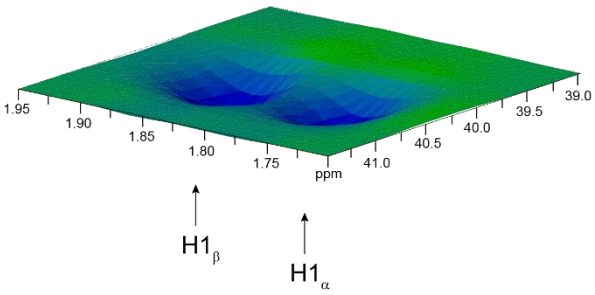

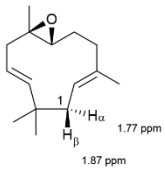

7

B) (*R*)-(1-^{13}C,1-^{2}H)FPP

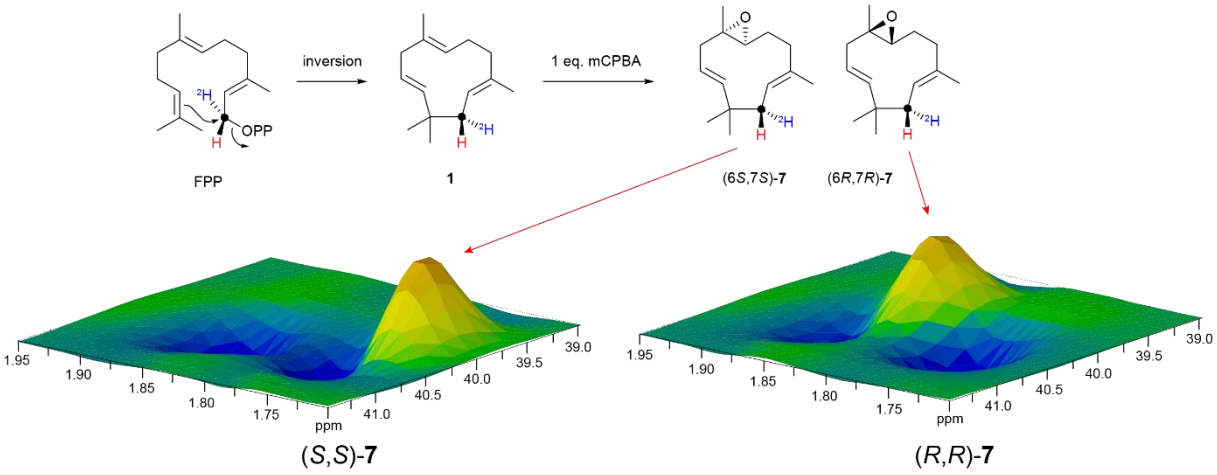

C) (*S*)-(1-^{13}C,1-^{2}H)FPP

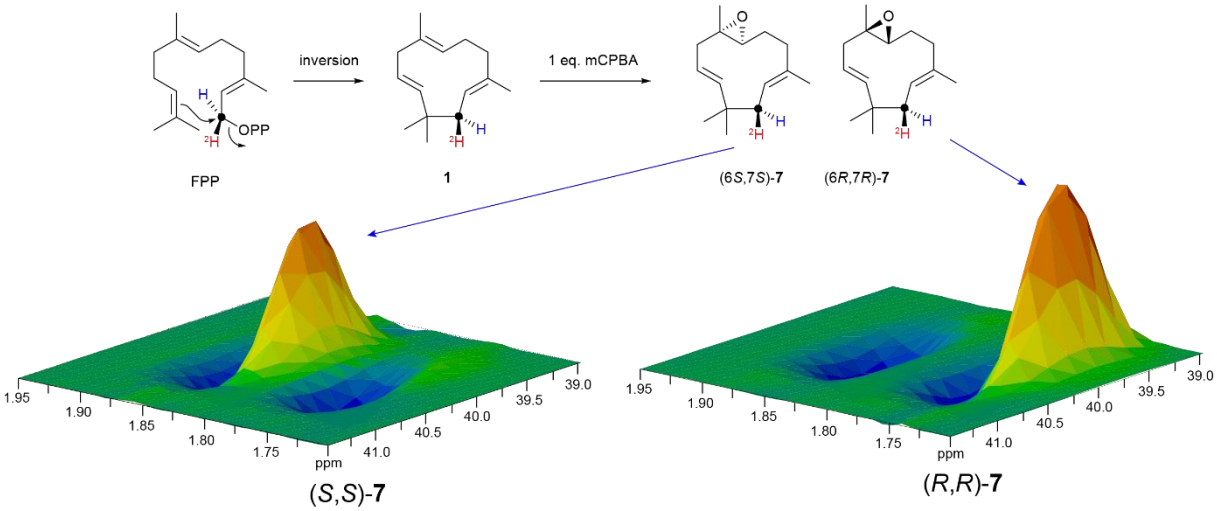

Figure S25. Inversion of configuration at C1. Partial HSQC spectra of A) unlabelled **7** showing crosspeaks for the two diastereotopic hydrogens at C1 (signals down for CH_2 groups), B) (*S*,*S*)-**7** and (*R*,*R*)-**7** from (*R*)-(1-^{13}C,1-^{2}H)FPP mixed with unlabelled **7**, and C) (*S*,*S*)-**7** and (*R*,*R*)-**7** from (*S*)-(1-^{13}C,1-^{2}H)FPP mixed with unlabelled **7**. In B) and C) the signals pointing down are from unlabelled **7** (CH_2 groups) and the signals pointing up are from labelled **7** (CH^2H groups), showing a slight upfield shift in both dimensions resulting from a deuterium isotope effect.

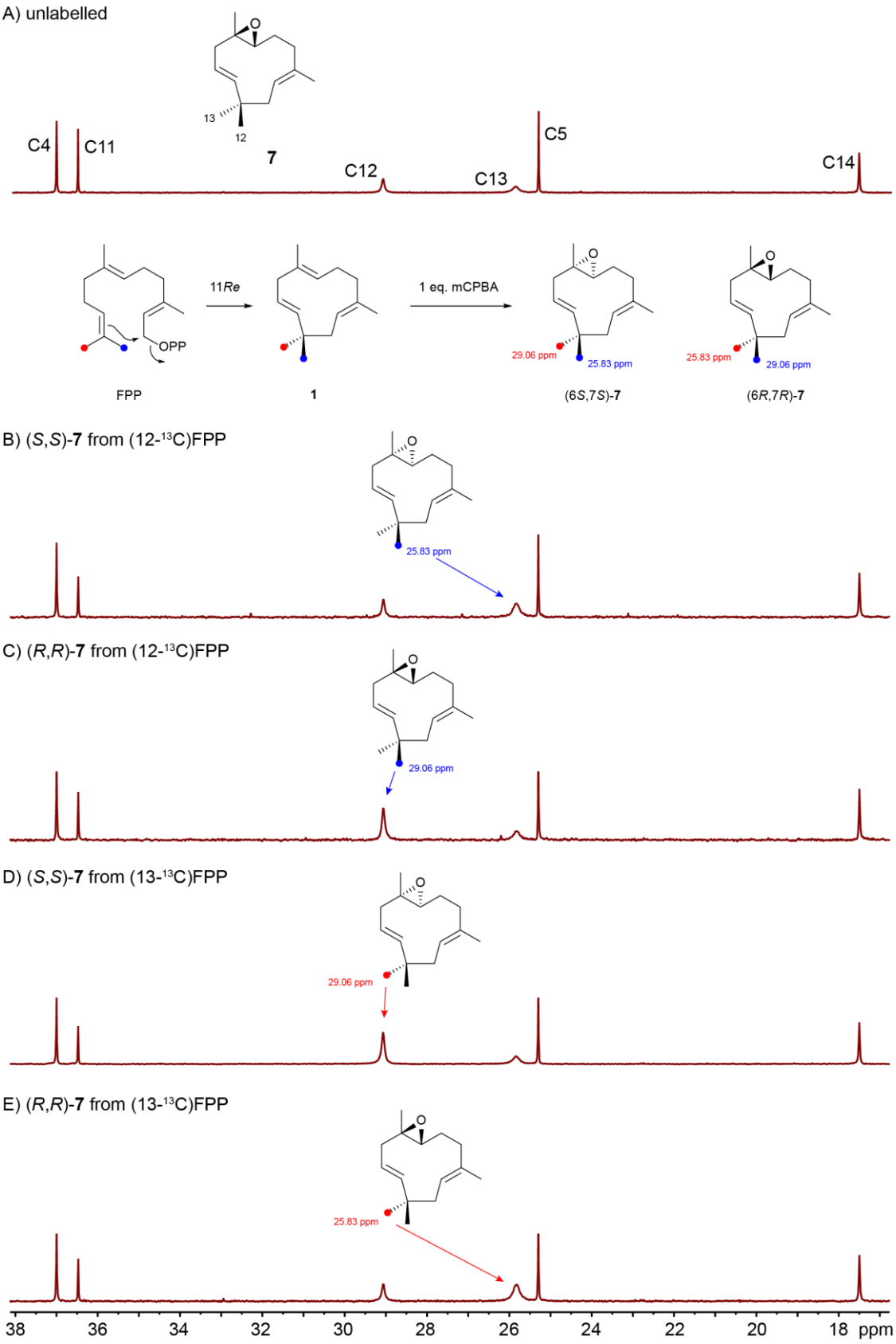

Figure S26. *Re* face attack at C11. Partial ^{13}C-NMR spectra of A) unlabelled **7**, B) (*S*,*S*)-**7** from (12-^{13}C)FPP mixed with unlabelled **7** (incorporation into δ = 25.83 ppm), C) (*R*,*R*)-**7** from (12-^{13}C)FPP mixed with unlabelled **7** (incorporation into δ = 29.06 ppm), D) (*S*,*S*)-**7** from (13-^{13}C)FPP mixed with unlabelled **7** (incorporation into δ = 29.06 ppm), and E) (*R*,*R*)-**7** from (13-^{13}C)FPP mixed with unlabelled **7** (incorporation into δ = 25.83 ppm).

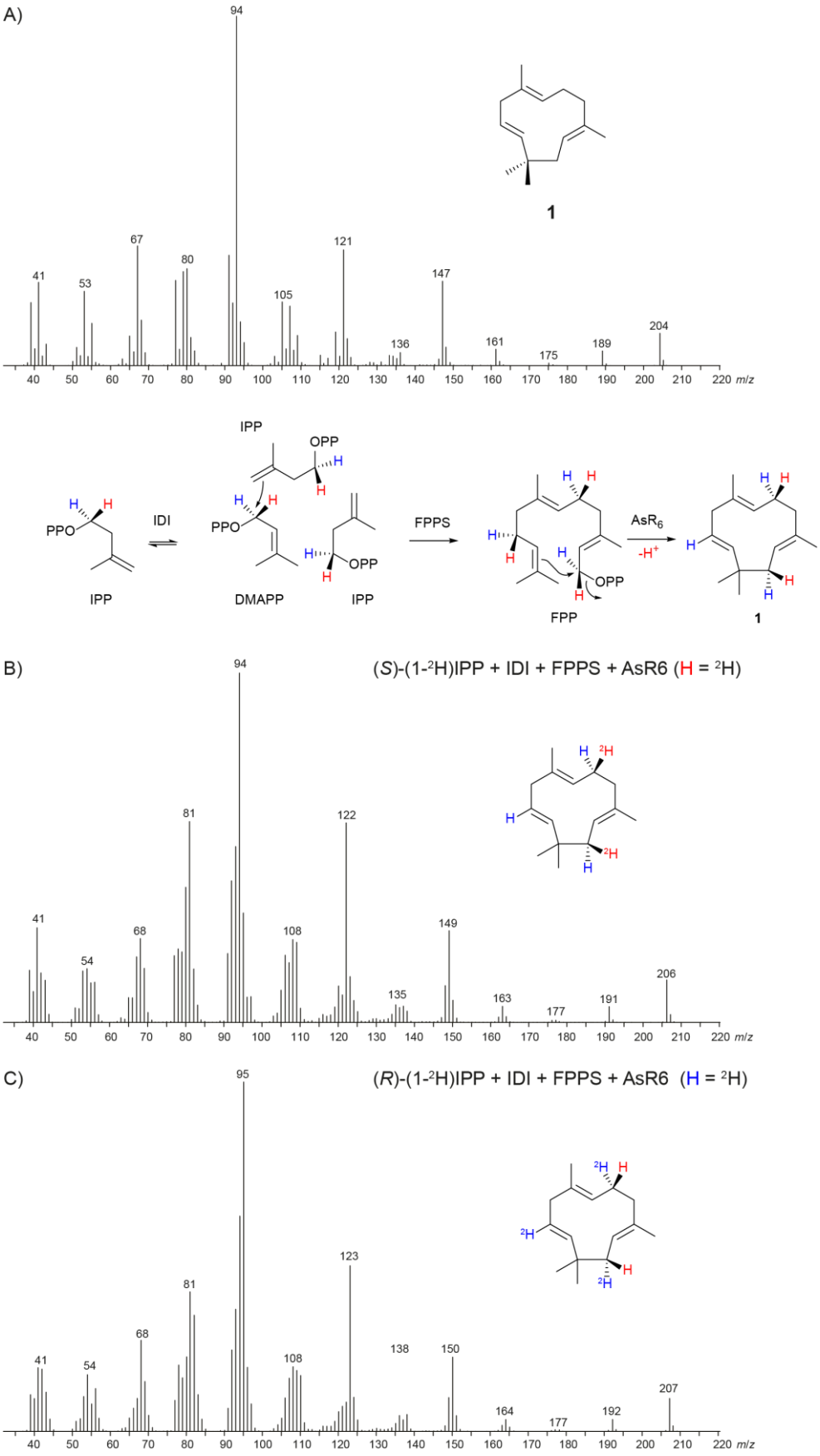

Figure S27. Deprotonation from C9. EI mass spectra of A) unlabelled **1**, B) ($^2H_2$)-**1** obtained with IDI, FPPS and AsR6 from (*S*)-(1-^{2}H)IPP, and C) ($^2H_3$)-**1** obtained with IDI, FPPS and AsR6 from (*R*)-(1-^{2}H)IPP.

References

1 N. P. Damodaran and S. Dev, *Tetrahedron*, 1968, **24**, 4123.

2 G. R. Fulmer, A. J. M. Miller, N. H. Sherden, H. E. Gottlieb, A. Nudelman, B. M. Stoltz, J. E. Bercaw and K. I. Goldberg, *Organometallics*, 2010, **29**, 2176.

3 C. Schotte, P. Lukat, A. Deuschmann, W. Blankenfeldt and R. J. Cox, *Angew. Chem. Int. Ed.*, 2021, **60**, online (doi: 10.1002/ange.202106718).

4 P. Rabe, J. Rinkel, E. Dolja, T. Schmitz, B. Nubbemeyer, T. H. Luu and J. S. Dickschat, *Angew. Chem. Int. Ed.*, 2017, **56**, 2776.

5 S. Schor, C. Schotte, D. Wibberg, J. Kalinowski and R. J. Cox, *Nat. Commun.*, 2018, **9**, 1963.

6 P. Rabe, L. Barra, J. Rinkel, R. Riclea, C. A. Citron, T. A. Klapschinski, A. Janusko and J. S. Dickschat, *Angew. Chem. Int. Ed.*, 2015, **54**, 13448.

7 J. Rinkel, L. Lauterbach and J. S. Dickschat, *Angew. Chem. Int. Ed.*, 2019, **58**, 452.

8 J. Rinkel and J. S. Dickschat, *Org. Lett.*, 2019, **21**, 2426.

9 P. Rabe, J. Rinkel, B. Nubbemeyer, T. G. Köllner, F. Chen and J. S. Dickschat, *Angew. Chem. Int. Ed.*, 2016, **55**, 15420.